Properties of the partonic phase at RHIC within PHSD

E. L. Bratkovskaya
Institute for Theoretical Physics, University of Frankfurt, Frankfurt, Germany
Frankfurt Institute for Advanced Study, Frankfurt, Germany
E-mail: Elena.Bratkovskaya@th.physik.uni-frankfurt.de

W. Cassing
Institute for Theoretical Physics, University of Giessen, Giessen, Germany

V. P. Konchakovski
Institute for Theoretical Physics, University of Giessen, Giessen, Germany
Bogolyubov Institute for Theoretical Physics, Kiev, Ukraine

O. Linnyk
Institute for Theoretical Physics, University of Giessen, Giessen, Germany

V. Ozvenchuk
Frankfurt Institute for Advanced Study, Frankfurt, Germany

V. Voronyuk
Joint Institute for Nuclear Research, Dubna, Russia
Frankfurt Institute for Advanced Study, Frankfurt, Germany
Bogolyubov Institute for Theoretical Physics, Kiev, Ukraine

Abstract. The dynamics of partons, hadrons and strings in relativistic nucleus-nucleus collisions is analyzed within the novel Parton-Hadron-String Dynamics (PHSD) transport approach, which is based on a dynamical quasiparticle model for partons (DQPM) matched to reproduce recent lattice-QCD results – including the partonic equation of state – in thermodynamic equilibrium. The transition from partonic to hadronic degrees of freedom is described by covariant transition rates for the fusion of quark-antiquark pairs or three quarks (antiquarks), respectively, obeying flavor current-conservation, color neutrality as well as energy-momentum conservation. In order to explore the space-time regions of 'partonic matter' the PHSD approach is applied to nucleus-nucleus collisions from SPS to RHIC energies. Detailed comparisons are presented for hadronic rapidity spectra and transverse mass distributions. The traces of partonic interactions are found in particular in the elliptic flow of hadrons as well as in an approximate quark-number scaling at the top RHIC energy.

1. Introduction

The 'Big Bang' scenario implies that in the first micro-seconds of the universe the entire state has emerged from a partonic system of quarks, antiquarks and gluons – a quark-gluon plasma (QGP) – to color neutral hadronic matter consisting of interacting hadronic states (and resonances) in which the partonic degrees of freedom are confined. The nature of confinement and the dynamics of this phase transition has motivated a large community for several decades and is still an outstanding question of todays physics. Early concepts of the QGP were guided by the idea of a weakly interacting system of partons which might be described by perturbative QCD (pQCD). However, experimental observations at the Relativistic Heavy Ion Collider (RHIC) indicated that the new medium created in ultrarelativistic Au+Au collisions is interacting more strongly than hadronic matter and consequently this concept had to be severely questioned. Moreover, in line with theoretical studies in Refs. [1, 2, 3] the medium showed phenomena of an almost perfect liquid of partons [4, 5] as extracted from the strong radial expansion and the scaling of elliptic flow $v_2(p_T)$ of mesons and baryons with the number of constituent quarks and antiquarks [4].

The question about the properties of this (nonperturbative) QGP liquid is discussed controversially in the literature and dynamical concepts describing the formation of color neutral hadrons from colored partons are scarce. A fundamental issue for hadronization models is the conservation of 4-momentum as well as the entropy problem because by fusion/coalescence of massless (or low constituent mass) partons to color neutral bound states of low invariant mass (e.g. pions) the number of degrees of freedom and thus the total entropy is reduced in the hadronization process [6, 7, 8]. This problem - a violation of the second law of thermodynamics as well as the conservation of four-momentum and flavor currents - has been addressed in Ref. [9] on the basis of the DQPM employing covariant transition rates for the fusion of 'massive' quarks and antiquarks to color neutral hadronic resonances or strings. In fact, the dynamical studies for an expanding partonic fireball in Ref. [9] suggest that the latter problems have come to a practical solution.

A consistent dynamical approach - valid also for strongly interacting systems - can be formulated on the basis of Kadanoff-Baym (KB) equations [10] or off-shell transport equations in phase-space representation, respectively [10, 11, 12]. In the KB theory the field quanta are described in terms of dressed propagators with complex selfenergies. Whereas the real part of the selfenergies can be related to mean-field potentials (of Lorentz scalar, vector or tensor type), the imaginary parts provide information about the lifetime and/or reaction rates of time-like 'particles' [13]. Once the proper (complex) selfenergies of the degrees of freedom are known the time evolution of the system is fully governed by off-shell transport equations (as described in Refs. [10, 13]). The determination/extraction of complex selfenergies for the partonic degrees of freedom has been performed before in Refs. [14, 15] by fitting lattice QCD (lQCD) 'data' within the Dynamical QuasiParticle Model (DQPM). In fact, the DQPM allows for a simple and transparent interpretation of lattice QCD results for thermodynamic quantities as well as correlators and leads to effective strongly interacting partonic quasiparticles with broad spectral functions. For a review on off-shell transport theory and results from the DQPM in comparison to lQCD we refer the reader to Ref. [13].

The actual implementations in the PHSD transport approach have been presented in detail in Refs. [16, 17]. Here we report again on the actual description of hadronization (Section 2). We also present results for rapidity distributions, transverse mass spectra and elliptic flow for heavy ion collisions at SPS (Section 3) and RHIC energies (Section 4) in comparison to data from the experimental collaborations.

2. Hadronization in PHSD

The hadronization, i.e. the transition from partonic to hadronic degrees of freedom, is described in PHSD by local covariant transition rates as introduced in Ref. [9] e.g. for $q + \bar{q}$ fusion to a meson m of four-momentum $p = (\omega, \mathbf{p})$ at space-time point $x = (t, \mathbf{x})$:

$$\begin{aligned}\frac{dN_m(x,p)}{d^4x d^4p} &= Tr_q Tr_{\bar{q}}\ \delta^4(p - p_q - p_{\bar{q}})\ \delta^4\left(\frac{x_q + x_{\bar{q}}}{2} - x\right) \\ &\times \omega_q\ \rho_q(p_q)\ \omega_{\bar{q}}\ \rho_{\bar{q}}(p_{\bar{q}})\ |v_{q\bar{q}}|^2\ W_m(x_q - x_{\bar{q}}, (p_q - p_{\bar{q}})/2) \\ &\times N_q(x_q, p_q)\ N_{\bar{q}}(x_{\bar{q}}, p_{\bar{q}})\ \delta(\text{flavor, color}). \end{aligned} \tag{1}$$

In Eq. (1) we have introduced the shorthand notation,

$$Tr_j = \sum_j \int d^4x_j \int \frac{d^4p_j}{(2\pi)^4}\ , \tag{2}$$

where $\sum_j$ denotes a summation over discrete quantum numbers (spin, flavor, color); $N_j(x,p)$ is the phase-space density of parton j at space-time position x and four-momentum p. In Eq. (1) δ(flavor, color) stands symbolically for the conservation of flavor quantum numbers as well as color neutrality of the formed hadron m which can be viewed as a color-dipole or 'pre-hadron'. Furthermore, $v_{q\bar{q}}(\rho_p)$ is the effective quark-antiquark interaction from the DQPM (displayed in Fig. 10 of Ref. [15]) as a function of the local parton $(q + \bar{q} + g)$ density ρ_p (or energy density). Furthermore, $W_m(x,p)$ is the dimensionless phase-space distribution of the formed 'pre-hadron', i.e.

$$W_m(\xi, p_\xi) = \exp\left(\frac{\xi^2}{2b^2}\right)\ \exp\left(2b^2(p_\xi^2 - (M_q - M_{\bar{q}})^2/4)\right) \tag{3}$$

with $\xi = x_1 - x_2 = x_q - x_{\bar{q}}$ and $p_\xi = (p_1 - p_2)/2 = (p_q - p_{\bar{q}})/2$. The width parameter b is fixed by $\sqrt{\langle r^2 \rangle} = b = 0.66$ fm (in the rest frame) which corresponds to an average rms radius of mesons. We note that the expression (3) corresponds to the limit of independent harmonic oscillator states and that the final hadron-formation rates are approximately independent of the parameter b within reasonable variations. By construction the quantity (3) is Lorentz invariant; in the limit of instantaneous 'hadron formation', i.e. $\xi^0 = 0$, it provides a Gaussian dropping in the relative distance squared $(\mathbf{r}_1 - \mathbf{r}_2)^2$. The four-momentum dependence reads explicitly (except for a factor 1/2)

$$(E_1 - E_2)^2 - (\mathbf{p}_1 - \mathbf{p}_2)^2 - (M_1 - M_2)^2 \leq 0 \tag{4}$$

and leads to a negative argument of the second exponential in (3) favoring the fusion of partons with low relative momenta $p_q - p_{\bar{q}} = p_1 - p_2$.

Related transition rates (to Eq. (1)) are defined for the fusion of three off-shell quarks $(q_1 + q_2 + q_3 \leftrightarrow B)$ to color neutral baryonic (B or $\bar{B}$) resonances of finite width (or strings) fulfilling energy and momentum conservation as well as flavor current conservation using Jacobi coordinates (cf. Ref. [16]).

On the hadronic side the PHSD transport approach includes explicitly the baryon octet and decouplet, the 0^-- and 1^--meson nonets as well as selected higher resonances as in HSD [18]. Hadrons of higher masses (> 1.5 GeV in case of baryons and > 1.3 GeV in case of mesons) are treated as 'strings' (color-dipoles) that decay to the known (low-mass) hadrons according to the JETSET algorithm [19]. We discard an explicit recapitulation of the string decay and refer the reader to the original work [19] or Ref. [20].

3. Application to nucleus-nucleus collisions at SPS energies

In this Section we employ the PHSD approach to nucleus-nucleus collisions at moderate relativistic energies. It is of interest, how the PHSD approach compares to the HSD [18] model (without explicit partonic degrees-of-freedom) as well as to experimental data. In Fig. 1 we show the transverse mass spectra of π^-, K^+ and K^- mesons for 7% central Pb+Pb collisions at 40 and 80 A·GeV and 5% central collisions at 158 A·GeV in comparison to the data of the NA49 Collaboration [21]. Here the slope of the π^- spectra is only slightly enhanced in PHSD relative to HSD which demonstrates that the pion transverse motion shows no sizeable sensitivity to the partonic phase. However, the $K^{\pm}$ transverse mass spectra are substantially hardened with respect to the HSD calculations at all bombarding energies - i.e. PHSD is more in line with the data - and thus suggests that partonic effects are better visible in the strangeness-degrees of freedom. The hardening of the kaon spectra can be traced back to parton-parton scattering as well as a larger collective acceleration of the partons in the transverse direction due to the presence of repulsive vector fields for the partons. The enhancement of the spectral slope for kaons and antikaons in PHSD due to collective partonic flow shows up much clearer for the kaons due to their significantly larger mass (relative to pions). We recall that in Refs. [22] the underestimation of the $K^{\pm}$ slope by HSD (and also UrQMD) had been suggested to be a signature for missing partonic degrees of freedom; the present PHSD calculations support this early suggestion. Moreover, the PHSD calculations for RHIC energies show a very similar trend - the inverse slope increases by including the partonic phase.

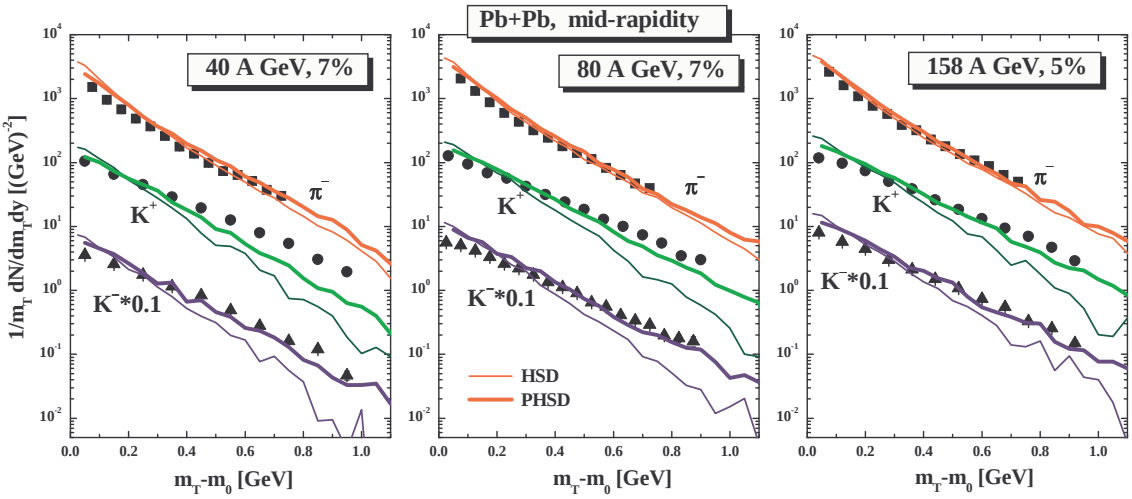

Figure 1. The π^-, K^+ and K^- transverse mass spectra for central Pb+Pb collisions at 40, 80 and 158 A·GeV from PHSD (thick solid lines) in comparison to the distributions from HSD (thin solid lines) and the experimental data from the NA49 Collaboration [21].

The strange antibaryon sector is of further interest since here the HSD calculations have always underestimated the yield [23]. Our detailed studies in Ref. [16] show that the HSD and PHSD calculations both give a reasonable description of the $\Lambda + \Sigma^0$ yield of the NA49 Collaboration [24]; both models underestimate the NA57 data [25] by about 30%. An even larger discrepancy in the data from the NA49 and NA57 Collaborations is seen for $(\bar{\Lambda} + \bar{\Sigma}^0)/N_{wound}$; here the PHSD calculations give results which are in between the NA49 data and the NA57 data whereas HSD underestimates the $(\bar{\Lambda} + \bar{\Sigma}^0)$ midrapidity yield at all centralities.

The latter result suggests that the partonic phase does not show up explicitly in an enhanced production of strangeness (or in particular strange mesons and baryons) but leads to a different redistribution of antistrange quarks between mesons and antibaryons. In fact, as demonstrated

in Ref. [16], we find no sizeable differences in the double strange baryons from HSD and PHSD – in a good agreement with the NA49 data – but observe a large enhancement in the double strange antibaryons for PHSD relative to HSD.

4. Application to nucleus-nucleus collisions at RHIC energies

In this section we continue the comparison of the PHSD transport approach to the experimental data from the RHIC collaborations as well as to the correspondent HSD results [17]. We find the rapidity distributions of the charged mesons to be slightly narrower in PHSD than those from HSD and actually closer to the experimental data. Also note that there is slightly more production of $K^{\pm}$ mesons in PHSD than in HSD while the number of charged pions is slightly lower. The actual deviations between the PHSD and HSD spectra are not dramatic but more clearly visible than at SPS energies (cf. Ref. [16]). Nevertheless, it becomes clear from Fig. 2 that the energy transfer in the nucleus-nucleus collision from initial nucleons to produced hadrons – reflected dominantly in the light meson spectra – is rather accurately described by PHSD. Fig. 2 also demonstrates that the longitudinal motion is well understood within the PHSD approach.

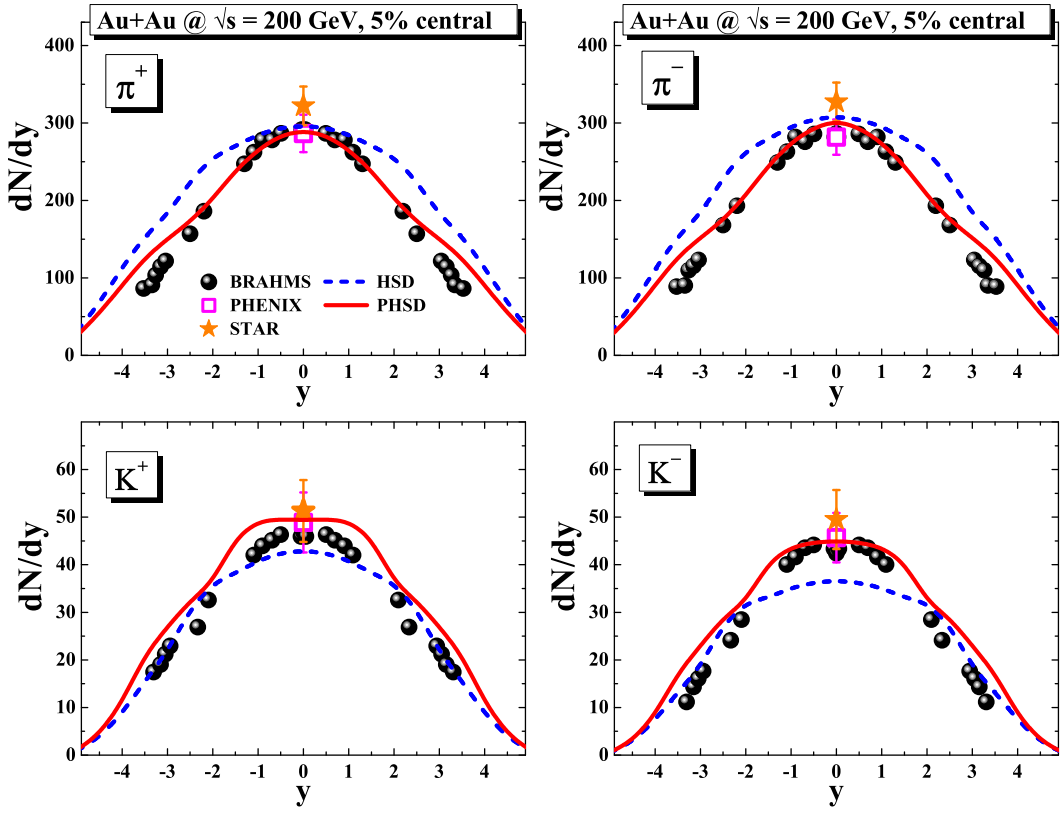

Figure 2. The rapidity distribution of π^+ (upper part, l.h.s.), K^+ (lower part, l.h.s.), π^- (upper part, r.h.s.) and K^- (lower part, r.h.s.) for 5% central Au+Au collisions at $\sqrt{s} = 200$ GeV from PHSD (solid red lines) in comparison to the distribution from HSD (dashed blue lines) and the experimental data from the RHIC Collaborations [26, 27, 28].

Independent information on the active degrees of freedom is provided by transverse mass spectra of the hadrons especially in central collisions. The actual results for RHIC energies are displayed in Fig. 3 where we show the transverse mass spectra of π^-, K^+ and K^- mesons for 5% central Au+Au collisions at $\sqrt{s} = 200$ GeV in comparison to the data of the RHIC

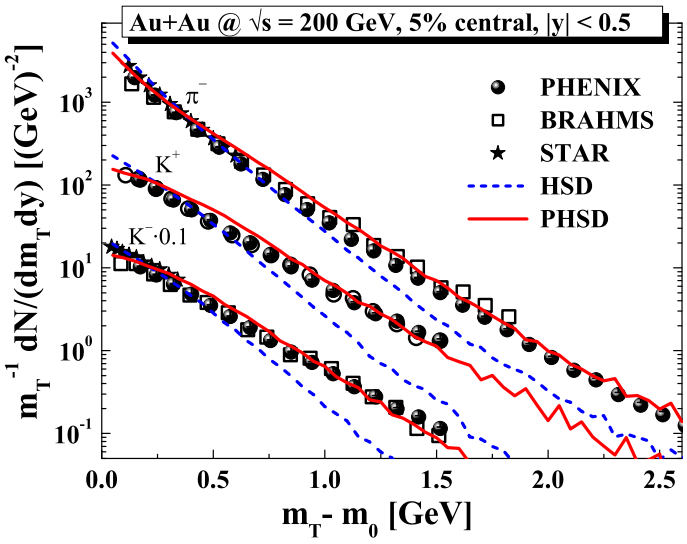

Figure 3. The π^-, K^+ and K^- transverse mass spectra for 5% central Au+Au collisions at $\sqrt{s}$ = 200 GeV from PHSD (solid red lines) in comparison to the distributions from HSD (dashed blue lines) and the experimental data from the BRAHMS, PHENIX and STAR Collaborations [26, 27, 28] at midrapidity.

Collaborations [26, 27, 28]. Here the slope of the π^- spectra is slightly enhanced in PHSD (solid red lines) relative to HSD (dashed blue lines) which demonstrates that the pion transverse mass spectra also show some sensitivity to the partonic phase (contrary to the SPS energy regime). The $K^\pm$ transverse mass spectra are substantially hardened with respect to the HSD calculations – i.e. PHSD is more in line with the data – and thus suggest that partonic effects are better visible in the strangeness degrees-of-freedom. The hardening of the kaon spectra can be traced back to parton-parton scattering as well as a larger collective acceleration of the partons in the transverse direction due to the presence of the repulsive mean-field for the partons. The enhancement of the spectral slopes for kaons and antikaons in PHSD due to collective partonic flow shows up much clearer for the kaons due to their significantly larger mass (relative to pions).

Of additional interest are the collective properties of the strongly interacting system which are explored experimentally via the elliptic flow

$$v_2(p_T, y) = \left\langle (p_x^2 - p_y^2)/(p_x^2 + p_y^2) \right\rangle |_{p_T,y} \tag{5}$$

of hadrons as a function of centrality, rapidity y, transverse momentum p_T or transverse kinetic energy per participating quarks and antiquarks. We note that the reaction plane in PHSD is given by the $x - z$ plane with the z-axis in beam direction.

We start in Fig. 4 with the elliptic flow v_2 (for Au+Au collisions at the top RHIC energy) as a function of the centrality of the reaction measured by the number of participating nucleons N_{part}. The solid (red) line stands for the results from PHSD which is compared to the data for charged particles from the PHOBOS Collaboration [30]. The dashed blue line refers to the corresponding results for v_2 from HSD (taken from Ref. [29]). The momentum integrated results in the pseudo-rapidity window $|\eta| \leq 1$ from PHSD compare well to the data from Ref. [30] whereas the HSD results clearly underestimate the elliptic flow as pointed out before in Ref. [29]. The relative enhancement of v_2 in PHSD with respect to HSD can be traced back to the high interaction rate in the partonic phase and to the repulsive mean field for partons. We note in

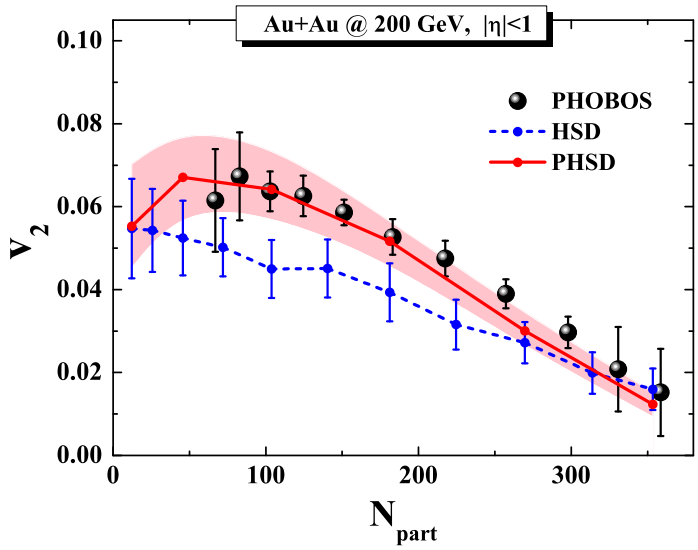

Figure 4. The elliptic flow v_2 for Au+Au collisions at the top RHIC energy $\sqrt{s} = 200$ GeV as a function of the centrality measured by the number of participating nucleons N_{part}. The solid (red) line stands for the results from PHSD whereas the dashed (blue) line represents the results from HSD (from Ref. [29]). The data are taken from the PHOBOS Collaboration [30] and correspond to momentum integrated events in the pseudo-rapidity window $|\eta| \leq 1$ for charged particles. The shaded band signals the statistical uncertainties of the PHSD calculations.

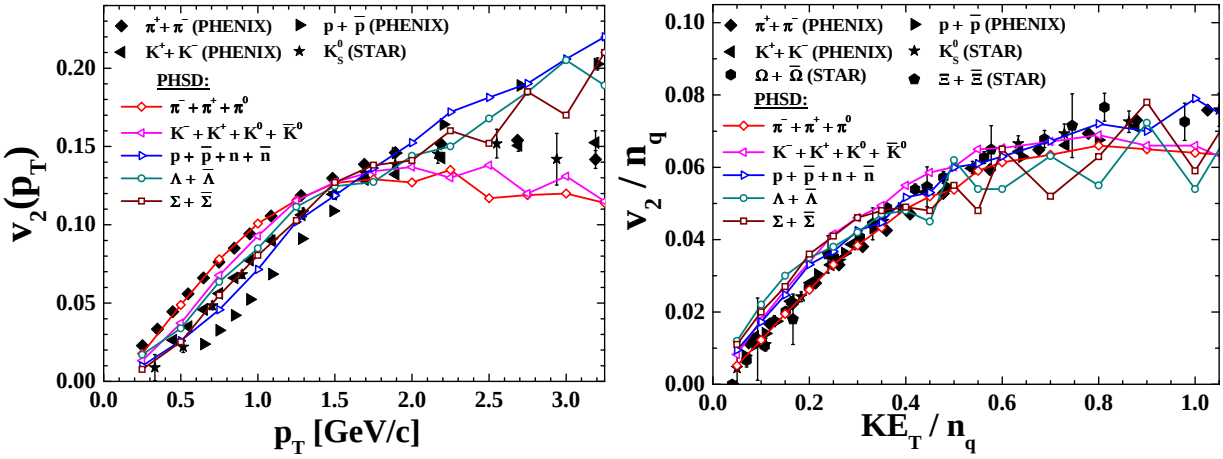

Figure 5. *Left:* The hadron elliptic flow v_2 for inclusive Au+Au collisions as a function of the transverse momentum p_T (in GeV) for different hadrons in comparison to the data from the STAR [31] and PHENIX Collaborations [32] within the same rapidity cuts. *Right:* The elliptic flow v_2 - scaled by the number of constituent quarks n_q - versus the transverse kinetic energy (6) divided by n_q for different hadron species in comparison to the data from the STAR [31] and PHENIX [32] Collaborations.

passing that PHSD calculations without mean fields only give a tiny enhancement for the elliptic flow relative to HSD.

Fig. 5 (l.h.s.) shows the final hadron v_2 versus the transverse momentum p_T for different

particle species in comparison to the data from the STAR [31] and PHENIX Collaborations [32]. We observe a mass separation in p_T as well as a separation in mesons and baryons for $p_T >$ 2 GeV roughly in line with data. The elliptic flow of mesons is slightly underestimated for $p_T > 2$ GeV in PHSD which is opposite to ideal hydrodynamics which overestimates v_2 at high transverse momenta. On the other hand, the proton (and antiproton) elliptic flow is slightly overestimated at low transverse momenta $p_T < 1.5$ GeV.

A further test of the PHSD hadronization approach is provided by the 'constituent quark number scaling' of the elliptic flow v_2 which has been observed experimentally in central Au+Au collisions at RHIC [4, 32, 33]. In this respect we plot v_2/n_q versus the transverse kinetic energy per constituent parton,

$$KE_T = \frac{m_T - m}{n_q} \ , \tag{6}$$

with m_T and m denoting the transverse mass and actual hadron mass, respectively. For mesons we have $n_q = 2$ and for baryons/antibaryons $n_q = 3$. The results for the scaled elliptic flow are shown in Fig. 5 (r.h.s.) in comparison to the data from the STAR [31] and PHENIX Collaborations [32] for different hadrons and suggest an approximate scaling. For $KE_T > 0.5$ GeV there is a tendency to underestimate the experimental measurements for $\Lambda, \Sigma, \bar{\Lambda}, \bar{\Sigma}$ baryons which we attribute to an underestimation of interaction terms in PHSD for high momentum hadrons. In this respect we recall that the momentum independence of the quasiparticle width γ and mass M is presently a rough approximation and has to be refined. Due to the limited statistics especially in the baryonic sector with increasing p_T this issue will have to be re-addressed with high statistics in future.

5. Summary

In this contribution we have addressed relativistic collisions of Pb+Pb at SPS energies and Au+Au collisions at RHIC energies in the PHSD approach which includes explicit partonic degrees of freedom as well as dynamical local transition rates from partons to hadrons (1). The hadronization process conserves four-momentum and all flavor currents and slightly increases the total entropy since the 'fusion' of rather massive partons dominantly leads to the formation of color neutral strings or resonances that decay microcanonically to lower mass hadrons. Since this dynamical hadronization process increases the total entropy the second law of thermodynamics is not violated (as is the case for simple coalescence models incorporating massless partons).

The PHSD approach has been also applied to nucleus-nucleus collisions from 40 to 160 A·GeV as well as for RHIC energies in order to explore the space-time regions of 'partonic matter' [16]. We have found that even central collisions at the top SPS energy of ∼158 A· GeV show a large fraction of non-partonic, i.e. hadronic or string-like matter, which can be viewed as a 'hadronic corona' [34]. This finding implies that neither purely hadronic nor purely partonic 'models' can be employed to extract physical conclusions in comparing model results with data. On the other hand - studying in detail Pb+Pb reactions at SPS energies in comparison to the data [16] - it is found that the partonic phase has only a very low impact on the longitudinal rapidity distributions of hadrons but a sizeable influence on the transverse-mass distribution of final kaons due to the partonic interactions. The most pronounced effect is seen on the production of multi-strange antibaryons due to a slightly enhanced $s\bar{s}$ pair production in the partonic phase from massive time-like gluon decay and a more abundant formation of strange antibaryons in the hadronization process. This enhanced formation of strange antibaryons in central Pb+Pb collisions at SPS energies by hadronization supports the early suggestion by Braun-Munzinger and Stachel [35, 36] in the statistical hadronization model - which describes well particle ratios from AGS to RHIC energies.

At RHIC energies the PHSD calculations show also a good reproduction of the hadron transverse mass and rapidity spectra. Furthermore, the elliptic flow v_2 is well described for

Au+Au reactions at $\sqrt{s} = 200$ GeV as a function of centrality as well as of transverse momenta up to $p_T \simeq 1.5$ GeV/c. Due to the local transition rates from partons to hadrons (1) the PHSD approach also gives approximate quark number scaling of the elliptic flow as found experimentally by the RHIC Collaborations.

Acknowledgements
Work supported in part by the HIC for FAIR framework of the LOEWE program and by DFG.

[1] E. Shuryak, Prog. Part. Nucl. Phys. 53 (2004) 273.
[2] M. H. Thoma, J. Phys. G 31 (2005) L7; Nucl. Phys. A 774 (2006) 307.
[3] A. Peshier and W. Cassing, Phys. Rev. Lett. 94 (2005) 172301.
[4] I. Arsene *et al.*, Nucl. Phys. A 757 (2005) 1; B. B. Back *et al.*, Nucl. Phys. A 757 (2005) 28; J. Adams *et al.*, Nucl. Phys. A 757 (2005) 102; K. Adcox *et al.*, Nucl. Phys. A 757 (2005) 184.
[5] T. Hirano and M. Gyulassy, Nucl. Phys. A 769 (2006) 71.
[6] R. C. Hwa and C. B. Yang, Phys. Rev. C 67 (2003) 034902; V. Greco, C. M. Ko and P. Levai, Phys. Rev. Lett. 90 (2003) 202302.
[7] R. J. Fries, B. Müller, C. Nonaka and S. A. Bass, Phys. Rev. Lett. 90 (2003) 202303.
[8] Z.-W. Lin *et al.*, Phys. Rev. C 72 (2005) 064901.
[9] W. Cassing and E. L. Bratkovskaya, Phys. Rev. C 78 (2008) 034919.
[10] S. Juchem, W. Cassing and C. Greiner, Phys. Rev. D 69 (2004) 025006; Nucl. Phys. A 743 (2004) 92.
[11] W. Cassing and S. Juchem, Nucl. Phys. A 665 (2000) 377; *ibid* A 672 (2000) 417.
[12] Y. B. Ivanov, J. Knoll and D. N. Voskresensky, Nucl. Phys. A 672 (2000) 313.
[13] W. Cassing, E. Phys. J. ST 168 (2009) 3.
[14] W. Cassing, Nucl. Phys. A 791 (2007) 365.
[15] W. Cassing, Nucl. Phys. A 795 (2007) 70.
[16] W. Cassing and E. L. Bratkovskaya, Nucl. Phys. A 831 (2009) 215.
[17] E. L. Bratkovskaya, W. Cassing, V. P. Konchakovski, O. Linnyk, Nucl. Phys. A 856 (2011) 162.
[18] W. Cassing and E. L. Bratkovskaya, Phys. Rep. 308 (1999) 65.
[19] H.-U. Bengtsson and T. Sjöstrand, Comp. Phys. Commun. 46 (1987) 43.
[20] T. Falter, W. Cassing, K. Gallmeister, and U. Mosel, Phys. Rev. C 70 (2004) 054609.
[21] C. Alt et al., NA49 Collaboration, Phys. Rev. C 66 (2002) 054902; Phys. Rev. C 77 (2008) 024903.
[22] E. L. Bratkovskaya, S. Soff, H. Stöcker, M. van Leeuwen, and W. Cassing, Phys. Rev. Lett. 92 (2004) 032302.
[23] J. Geiss, W. Cassing and C. Greiner, Nucl. Phys. A 644 (1998) 107.
[24] T. Anticic *et al.*, Phys. Rev. C 80 (2009) 034906.
[25] F. Antinori *et al.*, Phys. Lett. B 595 (2004) 68; J. Phys. G: Nucl. Phys. 32 (2006) 427.
[26] S. S. Adler *et al.*, Phys. Rev. C 69 (2004) 034909.
[27] J. Adams *et al.*, Phys. Rev. Lett. 92 (2004) 112301.
[28] I. G. Bearden *et al.*, Phys. Rev. Lett. 94 (2005) 162301.
[29] E. L. Bratkovskaya, W. Cassing, and H. Stöcker, Phys. Rev. C 67 (2003) 054905.
[30] B. B. Back *et al.*, Phys. Rev. C 72 (2005) 051901.
[31] J. Adams *et al.*, Phys. Rev. Lett. 92 (2004) 052302; Phys. Rev. Lett. 95 (2005) 122301.
[32] A. Adare *et al.*, Phys. Rev. Lett. 98 (2007) 162301.
[33] S. Afanasiev *et al.*, Phys. Rev. C 80 (2009) 024909.
[34] J. Aichelin and K. Werner, Phys. Rev. C79 (2009) 064907.
[35] P. Braun-Munzinger *et al.*, Phys. Lett. B 365 (1996) 1; *ibid.* B 465 (1999) 15; *ibid.* B 518 (2001) 41.
[36] A. Andronic, P. Braun-Munzinger and J. Stachel, Nucl. Phys. A 772 (2006) 167.